Differentiating a Ligand's Chemical Requirements for Allosteric Interactions from Those for Protein Binding. Phenylalanine Inhibition of Pyruvate Kinase[†,‡]

Rachel Williams, Todd Holyoak, Gissel McDonald, Chunshan Gui, and Aron W. Fenton*

Department of Biochemistry and Molecular Biology, The University of Kansas Medical Center, Kansas City, Kansas 66160

Received November 28, 2005; Revised Manuscript Received March 14, 2006

ABSTRACT: The isoform of pyruvate kinase from brain and muscle of mammals (M_1-PYK) is allosterically inhibited by phenylalanine. Initial observations in this model allosteric system indicate that Ala binds competitively with Phe, but elicits a minimal allosteric response. Thus, the allosteric ligand of this system must have requirements for eliciting an allosteric response in addition to the requirements for binding. Phe analogues have been used to dissect what chemical properties of Phe are responsible for eliciting the allosteric response. We first demonstrate that the L-2-aminopropanaldehyde substructure of the amino acid ligand is primarily responsible for binding to M_1-PYK. Since the allosteric response to Ala is minimal and linear addition of methyl groups beyond the β-carbon increase the magnitude of the allosteric response, we conclude that moieties beyond the β-carbon are primarily responsible for allostery. Instead of an all-or-none mechanism of allostery, these findings support the idea that the bulk of the hydrophobic side chain, but not the aromatic nature, is the primary determinant of the magnitude of the observed allosteric inhibition. The use of these results to direct structural studies has resulted in a 1.65 Å structure of M_1-PYK with Ala bound. The coordination of Ala in the allosteric amino acid binding site confirms the binding role of the L-2-aminopropanaldehyde substructure of the ligand. Collectively, this study confirms that a ligand can have chemical regions specific for eliciting the allosteric signal in addition to the chemical regions necessary for binding.

A linked equilibrium analysis of allosteric regulation quantifies the allosteric coupling independent of the initial substrate affinity and the initial effector affinity (*1*). As a result, a ligand may have chemical regions that contribute to binding to the protein but are not employed in the allosteric coupling; only selective chemical groups of the ligand might be responsible for eliciting the allosteric response. Thus, linkage concepts might provide a valuable framework for understanding the agonistic/antagonistic properties in drug/receptor studies.

The pyruvate kinase isozyme found in brain and muscle (M_1-PYK)[1] is one of four mammalian isozymes of pyruvate kinase (PYK), all of which catalyze the conversion of phospho(enol)pyruvate (PEP) and MgADP to pyruvate (Pyr) and MgATP. Phe is an allosteric inhibitor of M_1-PYK that causes a decrease in this enzyme's apparent affinity for PEP (*2*). The physiological relevance of this regulation is not fully understood but may have implications in phenylketonuria (*3−6*). Biochemically, the Phe inhibition of M_1-PYK from

rabbit has become a model system for the study of allosteric enzymes. The most extensive description of changes in protein properties associated with the binding of Phe has been provided by Lee and co-workers (e.g. *7−9*). However, at the onset of the current study the location of the allosteric amino acid binding site on the structure of PYK had not yet been identified.

Additions of Ala to Phe-inhibited M_1-PYK reverse the Phe inhibition (*2, 10, 11*). However, small amino acids have not previously been reported to elicit an allosteric response from this enzyme. On the basis of these observations of the comparative effects of Phe and Ala on M_1-PYK activity, we considered that Phe could be an example of an allosteric ligand that has chemical regions specific for allosteric functions in addition to those specific for binding.

The goal of the current work was to further distinguish the chemical regions of Phe responsible for binding to rabbit M_1-PYK and the chemical properties of the allosteric ligand that are responsible for eliciting the allosteric response. To overcome saturation limitations at pH 7.0, we demonstrate that Phe binds with a higher affinity at pH 9.0. At pH 9.0, we employ Phe analogues in combination with a linkage-analysis to probe the chemical group functions of Phe. The findings from analogue studies are further supported by a 1.65 Å structure of M_1-PYK with Ala bound.

MATERIALS AND METHODS

Materials. M_1-PYK purified from rabbit muscle was purchased from Roche Applied Science. Succinic acid and the potassium salt of PEP were purchased from Fluka.

---

* To whom correspondence should be addressed. E-mail: afenton@kumc.edu.

[1] Abbreviations: PYK, pyruvate kinase; M_1-PYK, the pyruvate kinase isozyme found in mammal brain and muscle; PEP, phospho(enol)pyruvate; Fru-1,6-BP, fructose-1,6-bisphosphate; Pyr, pyruvate.

NADH, L-lactic dehydrogenase (Type III bovine heart), sodium pyruvate, glycerol, Sephadex G-50, and the potassium salt of ADP were purchased from Sigma. Other buffer components were from Fisher Scientific.

Due to multiple names associated with many of the ligand analogues used in this study, we have chosen to use the commercial names as given by the supplier. For many of the analogues, the combination of low solubility and a low affinity to the allosteric binding site of M$_1$-PYK may have prevented an observed effect (we have constrained the current study to ligand solubility in aqueous buffers without the aid of organic solvents). Therefore, we indicate the concentration ranges of analogues that were used to test for allosteric effect (plain text in brackets) and competitive binding (*italicized text in brackets*). L-Phe [0−81 mM] was purchased from Fluka or Fisher Scientific. The L-forms of Ala [0−220 mM]-[*0−80 mM*], Arg [0−112 mM][*0−32 mM*], Asn [0−26 mM]-[*0−3.6 mM*], Asp [0−34 mM][*0−4.7 mM*], Cys [0−105 mM][*0−9 mM*], Gln [0−80 mM][*0−23mM*], Gly [0−230 mM][*0−50 mM*], Glu [0−73 mM][*0−10 mM*], His [0−45 mM][*0−6.4 mM*], Ile [0−64 mM][*0−9 mM*], Leu [0−52 mM][*0−7.4mM*], Lys [0−117 mM][*0−33 mM*], Met [0−133 mM][*0−19 mM*], Pro [0−150 mM][*0−41 mM*], Ser [0−60 mM][*0−20 mM*], Thr [0−130 mM][*0−9 mM*], Trp [0−8.3 mM][*0−1.2 mM*], Tyr [0−4.8 mM][*0−0.67 mM*], and Val [0−83 mM][*0−12 mM*] were purchased from Fisher Scientific. 2-phenylethylamine HCl [0−200 mM][*0−55 mM*], ethylamine [0−40 mM][*0−13 mM*], and isopropylamine [0−81 mM] were purchased from Sigma. (S)-(+)-2-Phenylglycine [0−40 mM][*0−5.6 mM*], L-homophenylalanine HCl [0−1.8 mM], 2-aminoisobutyric acid [0−193 mM][*0−109 mM*], 4-nitro-L-phenylalanine [0−3.8 mM], 3-phenylpropionic acid [0−141 mM][*0−20 mM*], butylamine [0−42 mM][*0−13 mM*], D/L-2-aminocaprylic acid [0−0.27 mM], N,N-dimethyl-L-phenylalanine [0−145 mM], and O-methyl-L-tyrosine [0−32 mM] were produced by Aldrich. N-Acetyl-L-phenylalanine [0−46 mM][*0−6.6 mM*], L-homoserine [0−170 mM][*0−75 mM*], L-(+)-2,3-diaminopropionic acid [0−99 mM][*0−31 mM*], L-(+)-2-aminobutyric acid [0−108 mM][*0−31* mM], S-(+)-2-amino-2-methyl-3-phenylpropionoic acid [0−77 mM][*0−11 mM*], D-phenylalanine [0−61 mM][*0−27 mM*], propionic acid [*0−36 mM*], and L-alanine methyl ester HCl [0−100 mM][*0−29 mM*] were purchased from Acros Organics. N-Methyl-L-phenylalanine HCl [0−15 mM][*0−2 mM*], L-phenylalanine methyl ester [0−150 mM], L-norvaline [0−62], L-norleucine [0−45 mM], N-methyl-L-alanine [*0−65 mM*], D-alanine [*0−116 mM*], 3-cyclohexyl-L-alanine [0−7.7 mM], D/L-2-aminoheptanoic acid [0−4.7 mM], and L-alaninol [0−160 mM][*0−180 mM*] were obtained from Fluka. N-Formyl-L-phenylalanine [0−11 mM]-[*0−1.5 mM*], N-formyl-L-alanine [*0−25 mM*], and N-acetyl-L-alanine [*0−21*] were purchased from MP Biomedicals.

Kinetic Assays. Activity measurements were carried out at 30 °C using a lactate dehydrogenase coupled assay. Reactions were in 350 μL of a Tris buffer containing 50 mM Tris-HCl, 10 mM MgCl$_2$, 0.1 mM EDTA, 0.18 mM NADH, 19.6 U/mL lactate dehydrogenase and 5 mM ADP. With the exception of the studies in which pH was varied, all experiments were at pH 9.0. PEP and effector ligand concentrations were varied as indicated. Stock solutions of PEP and effector ligand were adjusted to the proper pH before addition, and dilutions were in KCl to maintain

constant K$^+$ concentration. K$^+$ concentrations from additions of KOH and from counterions of ligands were summed and KCl was supplemented to a total K$^+$ concentration of 500 mM in all assays. The enzymatic reaction was initiated with PEP and monitored at 340 nm over time. Data were collected in a 96-well format using a Molecular Devices Spectramax Plus384 spectrophotometer. Initial rates were collected from the linear portion of the progress curve.

Phe inhibition alters the apparent affinity of M$_1$-PYK for PEP ($K_{app−PEP}$) without altering maximal velocity (V_{max}) and is, therefore, a K-type allosteric system. However, increasing concentrations of 2-phenylethylamine, L-alaninol, L-alanine methyl ester, and L-phenylalanine methyl ester decreased V_{max}. The mechanism by which these analogues altered V_{max} was not further investigated.

Data Analysis. Due the ability to derive thermodynamic values using steady-state data (*12*) and the utility of semi-high throughput data collection using 96-well plate UV/vis spectrophotometer, the initial velocity data was the primary data collected in this study. PEP titrations of initial rates (*v*) were fit to the Hill equation:

$$v = \frac{V_{max}[A]^n}{(K_{app})^n + [A]^n} \quad (1)$$

where V_{max} is maximum velocity, A is the varied ligand, K_{app} is the concentration of substrate that yields a rate equal to one-half V_{max}, and n is the Hill coefficient.

The n_{PEP} values collected at pH 9.0 increase from near 1 to 1.9 as Phe increased. In the same conditions, the n_{Phe} values increase from 1 in the absence of PEP to above 1.5 in the presence of PEP. Therefore plots of $K_{app−PEP}$ as a function of Phe concentration were fit to

$$K_{app−a} = K_a \left(\left\{ (K_{ix})^2 + 2K_{ix}[X] + \left(\frac{n_{(xx)}}{2-n_{(xx)}}\right)^2 [X]^2 \right\} \middle/ \right.$$
$$\left\{ (K_{ix})^2 + 2K_{ix}Q\left(\left(\frac{n_{(xx)}}{2-n_{(xx)}}\right)^2 \middle/ \left(\frac{n_{(xx/aa)}}{2-n_{(xx/aa)}}\right)^2\right)^{0.5} [X] + \right.$$
$$\left. \left. Q^2\left(\frac{n_{(xx)}}{2-n_{(xx)}}\right)^2 [X]^2 \right\} \right)^{0.5} \quad (2)$$

in order to account for homotropic cooperative ligand binding (*1*). In eq 2, K_a is $K_{app−a}$ in the absence of X, K_{ix} is the dissociation constant for X in the absence of A, Q is the coupling constant between X and A, $n_{(xx)}$ is the Hill number for the response to X in the absence of A; and $n_{(xx/aa)}$ is the Hill number for the response to X in the presence of saturating A. Due to the number of parameters in eq 2, large errors in the fit parameters were often obtained when fitting to the full equation. Fits were improved by constraining $n_{(xx)−Phe}$ to 1 and $n_{(xx/aa)−Phe/PEP}$ to 1.5, values based on those experimentally determined as listed above. Therefore, these constraints have been made throughout this work. In a log−log plot of $K_{app−a}$ as a function of the concentration of X, Q is the difference between the upper and the lower plateaus. Equation 2 describes the allosteric communications in a dimer with one active site and one allosteric site per monomer (*1*). Unfortunately, the equivalent equation to describe a tetramer does not reduce. Since n_{Phe} values (in the presence vs absence of PEP) determine the steepness of
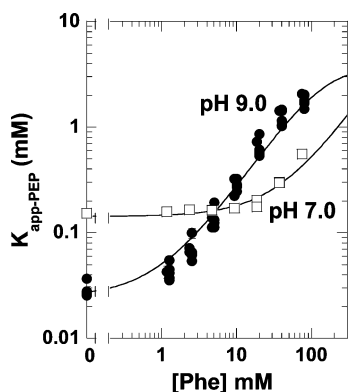
FIGURE 1: Effects of Phe on the $K_{app-PEP}$ at pH 9.0 (●) and pH 7.0 (□). Lines represent the best fits to eq 2 and eq 3, respectively. When error bars are not apparent, they are smaller than the data point symbols.

the transition between the upper and lower plateaus in a dimer example (*1*), the deviation in the fit that is apparent in Figure 1 (pH 9.0) is likely to be explained by the application of the dimer derived equation to fit data from a tetrameric enzyme. Although the fit parameters are compared, the qualitative comparisons are sufficient to draw the conclusions reported in this manuscript.

The more extensive the allosteric inhibition is, the smaller Q becomes. When sufficient data cannot be collected to define the upper plateau (examples in this study are due to the limiting solubility of ligands), eq 2 can be reduced to eq 3 if $n_{(xx)}$ is 1 (as is the case for Phe binding to M_1-PYK in the absence of PEP):

$$K_{app-a} = K_a\left(1 + \frac{[X]}{K_{ix}}\right) \tag{3}$$

We have used two methods to evaluate $K_{ix-analogue}$ for Phe analogues at pH 9.0. If the analogue induced an allosteric inhibition, then the $K_{ix-analogue}$ could be determined by following the effects of the ligand on $K_{app-PEP}$ as has been demonstrated for Phe at pH 9.0. This approach also allowed for the quantification of Q for analogues that displayed allosteric effects.

In the second method, the determination of K_{ix-Phe} was repeated at varying concentrations of analogue. Equation 3 can describe competitive binding between A and X (*13*). Therefore, K_{ix-Phe} values plotted as a function of analogue concentration were fit to eq 3 to determine the $K_{ix-analogue}$. This second approach for the evaluation of $K_{ix-analogue}$ is demonstrated in Figure 3 for the competitive binding between Ala and Phe. For data with only small allosteric coupling, $Q > 0.1$, the $K_{ix-analogue}$ was determined by competition with Phe binding. Due to the experimental design, the maximum concentrations of analogues that could be used in competition studies were less than those used to determine if the analogue elicited an allosteric response. K_{ix} and Q values obtained for Phe analogues are reported in Tables 2 and 3.

Crystal Preparation. Crystals of the M_1-PYK:Pyr:K:Mn: Ala complex were grown by the vapor diffusion hanging drop method using conditions similar to those previously reported (*14*). Briefly, M_1-PYK was desalted into 10 mM HEPES (pH 6.0) and 100 mM KCl using a Sephadex G-50 syringe barrel column and the protein concentrated to 5 mg/ mL. The mother liquor solution consisted of 700 μL of 60
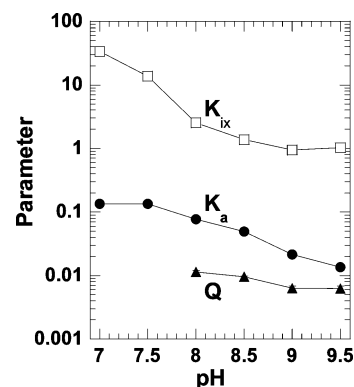

FIGURE 2: K_{ix-Phe} (□), K_{a-PEP} (●) and Q (▲) determined for the effects of Phe on $K_{app-PEP}$ as a function of pH. Q could not be determined at pH 7.0 and 7.5 since the upper plateau could not be determined and K_{ix} and K_a values at pH 7.0 and 7.5 were determined by fitting the data to eq 3. When error bars are not apparent they are smaller than the data point symbols.
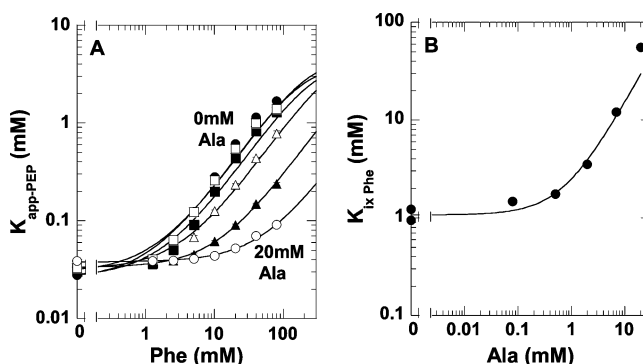

FIGURE 3: Competitive binding of Ala and Phe to M_1-PYK. A) $K_{app-PEP}$ as a function of Phe concentration at 0 mM (●), 0.08 mM (□), 0.5 mM (■), 2 mM (△), 7 mM (▲), and 20 mM (○) Ala. Data were fit to eq 2 or 3 to obtain K_{ix-Phe} values. B) The replot of K_{ix-Phe} values obtained in A as a function of Ala were fit to eq 3 to obtain K_{ix-Ala}. Lines represent best fits to the appropriate equations. When error bars are not apparent they are smaller than the data point symbols.

mM succinate (pH 5.5), 5.8 mM sodium pyruvate, 2.4 mM MnCl$_2$, 450 mM KCl, and a range of 18 to 20% PEG 8000. Crystals were observed to grow over a period of 3 days at room temperature from a solution of 2 μL of the well solution, 2 μL of the 5 mg/ml protein solution, and 0.5 μL of 1.5 M L-Ala. Crystals were cryoprotected by one of two methods. In the first method crystals were transferred to a 20 μL drop of 26.7 mM succinate pH 5.5, 2.6 mM sodium pyruvate, 1.1 mM MnCl$_2$, 200 mM KCl, 170 mM L-Ala, 22% PEG 8000 and 5% glycerol. The crystals were transferred to new drops containing increasing glycerol in 5% increments to a final concentration of 25%; all other buffer components were held constant. In the second method crystals were first transferred to new drops containing increasing pH to a final pH of 9.0, all other buffer components were as used in the first method. These crystals at pH 9.0 were transferred in stepwise fashion, as described above, to drops containing 25% glycerol. The crystals were cryocooled prior to data collection by immersion directly into liquid nitrogen. Data on cryocooled crystals maintained at 100 K were collected at Beamline X6A, NSLS, Brookhaven National Laboratory. No differences were observed between the structures solved on crystals soaked at pH 9.0 and those at pH 5.5 and only the pH 9.0 structure is reported here.

Molecular Replacement. The initial phases for rabbit muscle pyruvate kinase were obtained by the method of molecular replacement using the program MOLREP (*15*) encoded in the CCP4 suite (*16*). X-ray coordinates of the muscle pyruvate kinase tetramer (*14*), PDB entry 1F3W, was used as the search model after being stripped of all water molecules, ligands and ions. The molecular replacement solution resulted in an initial model with two tetramers in the asymmetric unit.

Structural Refinement. Refinement of the PK model was carried out in Refmac5 (*17*) encoded in the CCP4 suite. The refinement strategy consisted of an initial round of rigid-body refinement, followed by cycles of positional minimization and a final round of TLS refinement. After each round of refinement Fo-Fc and 2Fo-Fc electron-density maps were produced and manual model building/optimization was carried out using the model-building/map-fitting program Coot (*18*). The addition of ligands, metals and water molecules was also carried out using Coot prior to a final round of restrained refinement in Rafmac5. During the initial rounds of refinement, tight NCS restraints were utilized. In subsequent rounds of refinement medium NCS restraints were used on residues 115−175. In the final round of refinement all NCS restraints were removed. It has been reported that inclusion of TLS parameters gives improved refinement statistics (*19*). A final round of TLS refinement was carried out after the optimal number of TLS groups for each chain was determined on the TLSMD web server (http://skuld.bmsc.washington.edu/~tlsmd/). Due to limitations in Refmac5, only five TLS groups were used for each PK chain, for a total of 40 TLS groups. This resulted in a decrease in both R and R_{free} values from 16.1% and 19.3% to 14.8% and 17.4%, respectively. The final data and model statistics are summarized in Table 1.

RESULTS AND DISCUSSION

pH Dependence of K_a, K_{ix}, and Q. Figure 1 compares the response of $K_{app-PEP}$ as a function of Phe concentration at pH 7.0 and 9.0. At pH 7.0, the curve is shifted to the right, indicating that the affinity for Phe is reduced as compared to that at pH 9.0. As a result, no indication of saturation by Phe (upper plateau) is visible at pH 7.0 and Q cannot be estimated. Also apparent is that the affinity for PEP in the absence of Phe (vertical placement on the left *y*-axis) is increased at pH 9.0.

The dependence of K_a, K_{ix}, and Q on pH is demonstrated in Figure 2. Q could only be determined at pH values greater than 8.0, but over the pH range of 8.0 to 9.5 there does not appear to be a large change in this parameter. Thus, the communications between the allosteric binding site and the active site, as monitored by Q, are relatively insensitive to pH. In contrast, the binding affinities of PEP and Phe are both sensitive to pH. We assume, therefore, that data collected at pH 9.0 will be sufficiently informative to understanding the allosteric regulation of M_1-PYK by Phe. Accordingly, the remaining experiments reported in this work were performed at pH 9.0.

Binding of Allosteric Ligands. For analogues that elicit an allosteric response, $K_{ix-analogue}$ values were obtained from data fits using eq 2 or 3 as described in Materials and Methods (Table 2). Affinities of amino acid analogues that

Table 1: Data and Model Statistics for M_1-PYK:Pyr:K:Mn:Ala 1.65 Å Structure

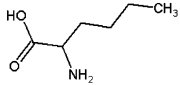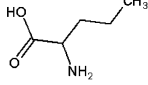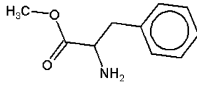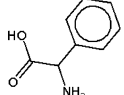|	
beam line	BNL-X6A
wavelength	0.9795 Å
space group	P 1
unit cell	a = 82.6, b = 109.0, c = 144.5 (Å)
	α = 95.2, β = 93.5, γ = 112.3 (°)
resolution limits	76.5−1.65 Å
unique reflections	508,412
completeness[a] (%; all data)	92.1 (55.2)
redundancy[a]	3.8 (3.3)
$I/\sigma_{(I)}$[a]	17.1 (4.3)
R_{merge}[a,b]	0.08 (0.28)
molecules/ASU	8
solvent content	44.4%
amino acids residues	4176
water molecules	4794
Mn^{2+}	8
K^+	8
Na^+	11
R_{work}[c]	14.8%
R_{free}[d]	17.4%
average B Factor	15.5 Å^2
Luzzati coordinate error	0.195Å
bond length RMSD	0.01Å
bond angle RMSD	1.15°
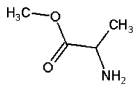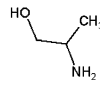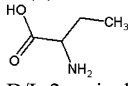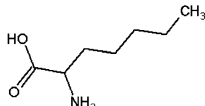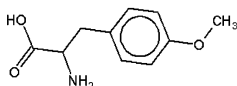
[a] Values in parentheses represent statistics for data in the highest resolution shells. The highest resolution shell comprises data in the range of 1.71−1.65 Å. [b] $R_{merge} = \sum_{hkl}\sum_i |I^i_{hkl} - \langle I_{hkl}\rangle|/\sum_{hkl} \sum_i I^i_{hkl}$ here *I* is the ith observation of a reflection with index *hkl* and the angle brackets indicate an average over all *i* observations. [c] R_{work} where $\sum_{hkl}|F^C_{hkl} - F^O_{hkl}|/\sum_{hkl}F^O_{hkl}$ where F^C_{hkl} is the magnitude of the calculated structure factor with index *hkl* and is F^O_{hkl} the magnitude of the observed structure factor with index *hkl*. [d] R_{free} was calculated as R_{work}, where F^O_{hkl} values were taken from a set of 25 590 reflections (5% of the data) that were not included in the refinement (*20*).

induced little or no allosteric effects on apparent PEP affinity were determined by competitive binding with Phe (Table 3). This approach is demonstrated in Figure 3. More complete tables showing analogue structures are included in the Supporting Information.

In Figure 3B there is no evidence for the formation of an upper plateau. This is consistent with competitive binding between Ala and Phe and there is no available data that suggests Ala and Phe bind to different binding sites and influence each other's binding allosterically (*11*). Gly binds competitively with Phe (Table 3). However, the addition of a β-methyl group (Ala) greatly increases ligand affinity (Table 3). Therefore, Ala seems to contain the requirements for binding and some chemical property beyond the β-methyl group is primarily responsible for eliciting the allosteric response.

No binding was detected for Phe and Ala analogues that have additions to the amino group (propionic acid, *N*-methyl-L-alanine, *N*-formyl-L-alanine, *N*-acetyl-L-alanine, 3-phenyl-propionic acid, *N*-methyl-L-phenylalanine, *N*-formyl-L-phenylalanine, *N*-acetyl-L-phenylalanine, and *N,N*-dimethyl-phenylalanine). The single exception to this was Pro. In agreement with earlier studies (*11*), no binding was apparent for the D-forms of Phe or Ala. The ability to accommodate replacements of the α-hydrogen with other chemical groups was not conclusive. Replacing the α-hydrogen by a methyl group has a relatively small effect on the affinity in the absence of the phenyl group (Ala vs 2-aminoisobutyric acid). However, in the presence of the phenyl group, this same replacement removes all evidence of binding (Phe vs *S*-(+)-
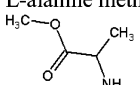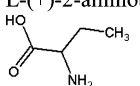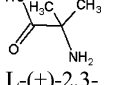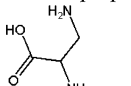
Table 2: Fit Parameters for Phe and Ala Analogues That Elicit Allosteric Effects[a]

Commercial Name	K_{ix} (mM)[b]	Q
Common amino acids; alphabetically		
L-alanine	-	0.53±0.01
L-isoleucine	4.7±0.2	No Upper Plateau
L-methionine	8.5±0.3	0.015±0.002
L-phenylalanine	1.06±0.01	0.0064±0.0005
L-proline	-	0.33±0.03
L-valine	8.1±0.3	No Upper Plateau
Uncommon amino acid analogs; alphabetically		
L-alanine methyl ester	-	0.37±0.03
L-alaninol	-	0.37±0.07
L-(+)-2-aminobutyric acid	-	0.37±0.01
D/L-2-aminoheptanoic acid[c]	0.75±0.07	No Upper Plateau
O-methyl-L-tyrosine	4.6±0.2	No Upper Plateau
L-norleucine	0.78±0.07	0.0078±0.0009
L-norvaline	61±6	No Upper Plateau
L-phenylalanine methyl ester	0.32±0.02	0.0050±0.0003
(S)-(+)-2-phenylglycine	54±3	No Upper Plateau

[a] K_{a-PEP} is 0.025±0.001 mM. [b] For analogues that induced a Q greater than 0.1, $K_{ix-analogue}$ values were determined by competition with Phe and are listed in Table 3. [c] For racemic mixtures, effects are assumed to be due to the L-form, and data are reported in terms of the L-form concentration.

Table 3: Ligand Affinity Values As Determined by Competitive Binding with Phe

Commercial Name	K_{ix} (mM)
Common Amino Acids; Alphabetically	
L-alanine	0.83±0.02
L-cysteine	0.43±0.01
L-glycine	44±2
L-methionine	14.2±0.6
L-proline	38±1
L-serine	0.455±0.006
L-threonine	3.85±0.09
Uncommon Amino Acid Analogs; Alphabetically	
L-alanine methyl ester	1.05±0.03
L-alaninol	17.8±0.3
L-(+)-2-aminobutyric acid	0.97±0.04
2-aminoisobutyric acid	2.1±0.1
L-(+)-2,3-diaminopropionic acid	20±2
isopropylamine	14.0±0.7

The methyl ester derivative of Ala (L-alanine methyl ester) did not interfere with ligand binding. Therefore, the negative charge of the carboxyl does not appear to play a major role in binding. However, removal of the carboxyl group (ethylamine) abolished detectable binding. Replacing the carboxyl group with a methyl group or a methyl alcohol group (isopropylamine and L-alaninol, respectively) greatly reduced binding affinity, but there is very little difference between the affinities of M_1-PYK for the two ligands containing these replacements. The same data trends were apparent with Phe analogues (butylamine, L-phenylalanine methyl ester, and 2-phenylethylamine). Collectively, these results could be consistent with a dependence of ligand binding affinity on the planer geometry of the ligand's carboxyl group oxygens. However, a second explanation consistent with these results is that the binding role of the ligand carboxyl group is isolated to the aldehyde oxygen. The latter possibility is most consistent with the structural data presented below that show hydrogen bonds between the carbonyl oxygen of the amino acid ligand and both the Nε2 nitrogen of H463 (3.24 Å) and the NH1 amino group of R105 (3.14 Å) (Figure 6). Taken together, the data support that the L-2-aminopropanaldehyde sub-structure of the amino acid ligands is primarily responsible for binding to M_1-PYK.

Triggering the Allosteric Signal. The allosteric response to Ala is small, and initially we did not consider Ala to be an allosteric analogue. However, this Ala inhibition was

2-amino-2-methyl-3-phenylpropionic acid). Taken together, the allosteric binding site of M_1-PYK appears to be specific for L-amino acids, and the amino group of the ligand seems to contribute substantially to the binding affinity of the allosteric ligand. As shown below, these results are consistent with the short hydrogen bond (2.69 Å) between the amine nitrogen of the bound amino acid and the backbone carbonyl of I468 (Figure 6).
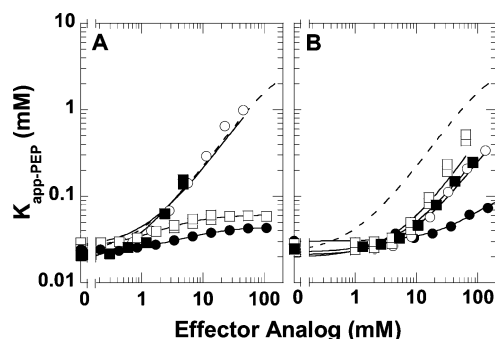
FIGURE 4: Apparent PEP affinity as a function of (A) amino acids with increasing lengths of linear carbon chains and that allosterically inhibit: Ala (●), 2-aminobutyric Acid (□), norleucine (○), and 2-aminoheptanoic acid (■); (B) the standard amino acids that show allosteric effects: Pro (●), Met (○), Ile (□), and Val (■). In each panel, the dashed line indicates the fit of Phe inhibition at pH 9.0 from Figure 1. Solid lines indicate the best fits to eq 2 or eq 3. When error bars are not apparent, they are smaller than the data point symbols. Corresponding fit parameters are listed in Tables 2 and 3.
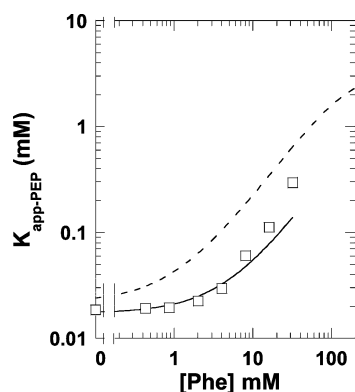

FIGURE 5: Apparent PEP affinities as a function of *O*-methyltyrosine. The dashed line indicates the fit of Phe inhibition at pH 9.0 from Figure 1. The solid line indicates the best fits to eq 3. Error bars are smaller than the data point symbols. Corresponding fit parameters are listed in Table 2.

reproducible (Figure 4A). We used this minimal response elicited by Ala ($Q = 0.53$) to define "no allosteric effect" as a Q less than 0.53 using up to 100 mM effector. Linear additions of carbons beyond the β-carbon (L-(+)-2-aminobutyric acid and L-norleucine) increase the allosteric inhibition, as indicated by smaller Q values (Figure 4A), when compared to Ala. This finding is not consistent with a consideration of allostery as all-or-none, as would be predicted by the two-state MWC model. No binding of long polar or charged amino acids (Arg, Asn, Asp, Gln, Glu, His, L-homoserine, and Lys) was detected. Consistent with previous studies (*11*), Pro, Met, Val, and Ile elicit allosteric responses (Figure 4B). Together, these results support the conclusion that the steric bulk, not aromaticity, of the hydrophobic side chain is most important for determining the magnitude of the allosteric inhibition.

Because Trp, Tyr, 4-nitro-phenylalanine, 3-cyclohexyl-L-alanine, D/L-2-aminocaprylic acid, and L-homophenylalanine have low solubility at pH 9.0, an evaluation of these compounds was not instructive. However, *O*-methyl-L-tyrosine elicits an allosteric inhibition that appears to be comparable to that of Phe (Figure 5). In addition, D/L-2-aminoheptanoic acid allosterically inhibits (Figure 4A). These results indicate that hydrophobic side chains larger than Phe

are able to trigger the allosteric inhibition. The maximum size of a hydrophobic side chain that can be accommodated is unknown. These data also do not address if, beyond a defined hydrophobic length of the side chain, additional hydrophilic and/or charge groups can be included.

In the absence of carbons beyond the β-carbon, polar (but not charged) groups can be accommodated at the β-carbon with little change in affinity (Ala vs Ser vs Cys vs L-(+)-2,3-diaminopropionic acid). When the γ-carbon is present, a polar group or a hydrophobic group at the β-carbon causes a decrease in affinity (L-(+)-2-aminobutyric acid vs Thr vs Val). In the presence of two carbons beyond the β-carbon, the addition of a methyl group at the β-carbon increases affinity (L-norvaline vs Ile). When a branch at the γ-carbon was introduced, affinity was decreased sufficiently that no binding was detected (L-norvaline vs Leu). Linear additions of hydrophobic carbons to the end of the side chain of L-norvaline increase binding affinity (L-norleucine and D/L-2-aminoheptanoic acid). Further support for altered ligand affinity upon modification of the amino acid side chain is apparent when comparing the natural amino acids. This sensitivity of K_{ix} to the chemical modifications of the side chain is consistent with a role of the side chain in eliciting the allosteric response.

The M_1−PYK:Pyr:K:Mn:Ala Structure. Most structures of mammalian PYK isozymes reported to date have been cocrystallized with a PEP analogue. This may imply that the presence of a PEP analogue aids crystal lattice formation. If true, then the relatively high magnitude of the inhibitory coupling between PEP and Phe affinities will provide a technical challenge for simultaneously saturating both the active and allosteric sites with the respective ligands. Therefore, cocrystallizing the ternary complex including Phe seems unlikely. There is sufficiently less coupling between PEP and an amino acid with a short hydrophobic side chain (Ala or 2-amino butyric acid). Obtaining crystals with both the PEP analogue and an amino acid that has a short hydrophobic side chain circumvents the technical difficulties present when using Phe. Using this knowledge, we have identified crystallization conditions that result in crystals of M_1-PYK when both Ala and pyruvate (a reaction product) are present. This approach is useful for identifying the amino acid binding site but is not necessarily valuable in characterizing protein changes associated with the allosteric inhibition.

The structure of PYK reported here represents the highest resolution structure of any PYK isozyme reported to date. The resulting model is of good quality with Procheck (*21*) analysis resulting in 93.5, 6.1, and 0.4% of the residues falling in the most favored, allowed, and generously allowed regions of the Ramachandran plot, respectively. One residue, E130 of chain B, falls in the disallowed region of the Ramachandran plot. As with other structures of M_1-PYK, the homotetramer consists of subunits that contain three main domains (A, B, and C domains); the N-terminus may be considered as a fourth domain. The location of the B-domain in the M_1-PYK:Pyr:K:Mn:Ala complex is different than either of the two orientations observed in the structure in the absence of Ala (1F3W). These multiple B-domain positions may support a structural ensemble (*7, 22*); an involvement of a B-domain rotation in the allosteric regulation (*23*) cannot be addressed since the structure with Phe has not been determined. The remaining domains and the
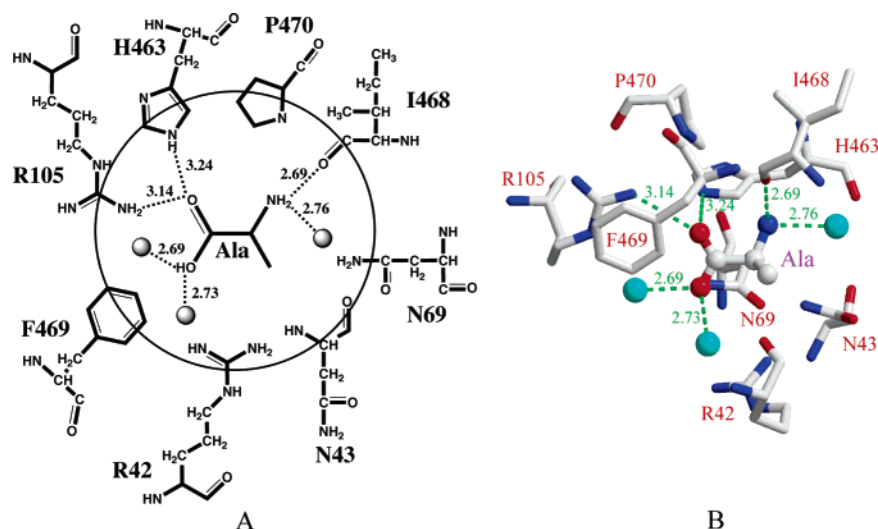
FIGURE 6: Schematic representation (A) and stick model (B) of the allosteric amino acid binding pocket showing hydrogen bonds formed between the bound Ala and protein residues, together with three water molecules (shown as gray spheres in A and cyan spheres in B).
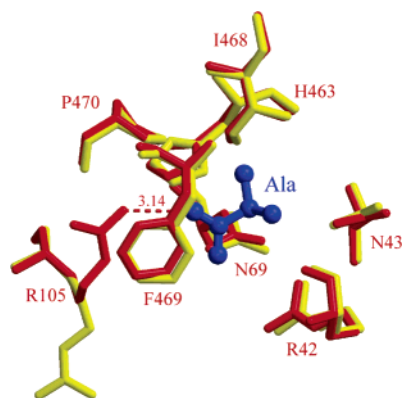

FIGURE 7: Conformational changes at the allosteric site with (red) and without (yellow, 1F3W) alanine bound (blue). The distance between the NH2 amine of R105 and the carbonyl oxygen of the bound alanine is also illustrated.

FIGURE 8: The Phe ligand that allosterically inhibits M_1-PYK has chemical region specific functions. The L-2-aminopropanaldehyde substructure of Phe (red) is primarily responsible for binding and the hydrophobic nature and size of the side chain elicits the allosteric response (green).

orientation of the monomers composing the tetramer are similar to the structures of the other known isozymes/complexes (1A49, 1A5U, 1AQF, 1F3W, 1F3X, and our model) (*14*, *24*, *25*). Superposing of a single monomer of 1F3W with the corresponding monomer in the reported structure results in a Cα RMSD between the two structures of only 0.51 Å.

Ala binds in a deep pocket between the A and C domains and distant from both the active site and the Fru-1,6-BP binding site identified in other isozymes. The rim of this pocket is surrounded by a number of positively charged residues. This ligand binding site is the same as that previously considered as a potential nucleotide binding site based on low resolution crystal soaks (*26*). Ala coordinates through hydrogen bonding with His463, Arg105, and the backbone carbonyl of Ile468 (Figure 6). This site is quite similar to the unliganded structure with the exception of Arg105 (Figure 7). Upon Ala binding, Arg105 adopts a conformation with its side chain extending toward the Ala ligand forming a hydrogen bond with one carboxylate oxygen of the bound Ala.

CONCLUSIONS

A linkage analysis of allosteric regulation (eq 2) quantifies the magnitude of the allosteric coupling (*Q*) independent of

K_a and K_{ix} (*1*). Therefore, there is a possibility (not a requirement) that only a specific chemical group of a ligand is involved in the allosteric regulation of a protein's affinity for a second ligand (*27*). It follows that modification of the allosteric specific moiety of the ligand might alter the magnitude of the allosteric response. Collectively, analogue studies in the current work support the conclusion that the L-2-aminopropanaldehyde substructure of amino acids is primarily responsible for binding to M_1-PYK and that the bulk of the hydrophobic side chain is most important for determining the magnitude of the allosteric inhibition (Figure 8).

The experiments using analogues in the current study were completed without a characterization of the ligand binding site on the structure of M_1-PYK. However, we have utilized the coupling information presented herein to direct cocrystallization studies. These studies have resulted in a structure of M_1-PYK cocrystallized with pyruvate and Ala, solved at a 1.65 Å resolution. The coordinating interactions between Ala and M_1-PYK (Figure 6) further support the binding role of the L-2-aminopropanaldehyde substructure.

From the results of the analogue studies, concluding what types of environments the phenyl ring of Phe might occupy is difficult. This difficulty is because as PEP binds, the binding energy of Phe to the enzyme must drive an increasingly unfavorable energetic coupling (inhibition) involving the phenyl ring. The phenyl ring might then be placed in an energetically favorable (likely hydrophobic) or unfavorable environment, either of which could elicit changes in the protein. Some clue to the protein environment to which the phenyl ring interacts might be gained by considering the K_{ix} values determined for those analogues that elicit allosteric
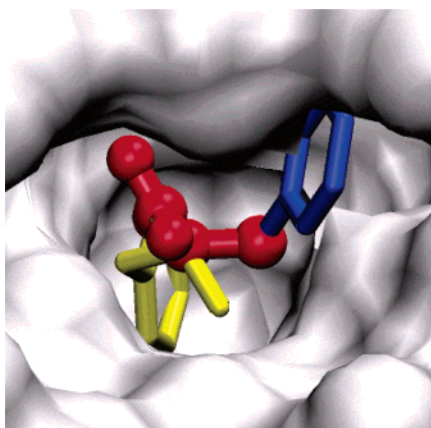
FIGURE 9: A surface representation of the allosteric amino acid binding site and two hypothetical Phe conformations (shown as blue and yellow sticks, respectively). Both of these two Phe rotomeric states would be accommodated in the binding pocket with no steric conflict with the protein. The bound Ala is shown in red ball-and-stick representation.

inhibition. The addition of a methyl group to Ala, 2-amino butyric acid, does not alter affinity. A second addition in aliphatic length (norvaline and Leu) greatly reduces affinity. Hydrophobic additions to the side chain that extend the length beyond that of norvaline decrease K_{ix}. Therefore, energetically favorable interactions of atoms beyond the length of norvaline might be compensating for the unfavorable interactions that occur with atoms at the intermediate length. Favorable interactions with the hydrophobic side chain that contribute to decreased K_{ix} is consistent with an interaction of the longer side chains with a hydrophobic site on the protein.

In our structure of M_1-PYK, the amino acid binding site has some vacancy which has not been occupied by Ala. This space should enable the site to accommodate much larger ligand than Ala, such as Phe. Figure 9 demonstrates that two Phe conformations with their backbone atoms fixed to the backbone of the bound Ala can bind in the amino acid binding site without a great steric conflict with the protein. It is of interest to note that one of these Phe conformations would position the phenyl ring of the ligand so that it would interact with both F469 and F501 that lie on the opposite side of the binding site. This could provide a mechanism for allosteric signal propagation that would be consistent with the thermodynamic studies that show a correlation between the hydrophobic nature of the effector side chain and the allosteric response.

Our conclusions do not support an all-or-none mechanism. In our studies, the protein has not been modified, and therefore, in the absence of effector, any potential equilibrium between potential conformations has not been perturbed. The presence of the upper plateaus at high concentrations of effectors (Figure 4) indicates saturation by effectors in the presence of bound substrate and therefore the formation of the ternary substrate−protein−effector complexes (*13*). Since the $K_{0.5-PEP}$ values for the upper plateaus obtained upon saturation with different effectors indicate different substrate affinities, the ternary complexes formed with the inhibitors are not equivalent. Our results are more consistent with an ensemble based description of each enzyme complex (*7, 22*) and a description of allostery that considers four enzyme complexes for each substrate/effector pair (*1*).

Finally, we have illuminated an example of the linkage based consideration that a specific chemical group of a ligand may be involved in the allosteric regulation. This consideration may provide a theoretical basis to explain a number of "partial allosteric effects" and agonistic/antagonistic effects reported for other systems. Furthermore, an understanding that only a select region of an allosteric ligand may contribute to determining the magnitude of the allosteric response will aid in drug design; examples might include designing competitive ligands that do not elicit an allosteric response or allosteric ligands that bind selectively to only one isozyme.

SUPPORTING INFORMATION AVAILABLE

Tables S-1, S-2, and S-3 in the Supporting Information present a more complete representation of analogue structures used in the current study. The obtained fit parameters for each analogue are also included. This material is available free of charge via the Internet at http://pubs.acs.org.

REFERENCES

1. Reinhart, G. D. (2004) Quantitative analysis and interpretation of allosteric behavior, *Methods Enzymol. 380*, 187−203.
2. Carminatti, H., Jimenez de Asua, L., Leiderman, B., and Rozengurt, E. (1971) Allosteric properties of skeletal muscle pyruvate kinase, *J. Biol. Chem. 246*, 7284−7288.
3. Feksa, L. R., Cornelio, A. R., Dutra-Filho, C. S., Wyse, A. T. S., Wajner, M., and Wannmacher, C. M. D. (2003) Characterization of the inhibition of pyruvate kinase caused by phenylalanine and phenylpyruvate in rat brain cortex, *Brain Res. 968*, 199−205.
4. Feksa, L. R., Cornelio, A. R., Rech, V. C., Dutra-Filho, C. S., Wyse, A. T. S., Wajner, M., and Wannmacher, C. M. D. (2002) Alanine prevents the reduction of pyruvate kinase activity in brain cortex of rats subjected to chemically induced hyperphenylalanineamia, *Neurochem. Res. 27*, 947−952.
5. Miller, A. L., Hawkins, R. A., and Veech, R. L. (1973) Phenylketonuria: phenylalanine inhibits brain pyruvate kinase *in vivo*, *Science 179*, 904−906.
6. Weber, G. (1969) Inhibition of human brain pyruvate kinase and hexokinase by phenylalanine and phenylpyruvate: possible relevance to phenylketonuric brain damage, *Proc. Natl. Acad. Sci. U.S.A. 63*, 1365−1369.
7. Yu, S., Lee, L. L.-Y., and Lee, J. C. (2003) Effects of metabolites on the structural dynamics of rabbit muscle pyruvate kinase, *Biophys. Chem. 103*, 1−11.
8. Consler, T. G., Jennewein, M. J., Cai, G.-Z., and Lee, J. C. (1990) Synergistic effects of proton and phenylalanine on the regulation of muscle pyruvate kinase, *Biochemistry 29*, 10765−10771.
9. Consler, T. G., Woodward, S. H., and Lee, J. C. (1989) Effects of primary sequence differences on the global structure and function of an enzyme: a study of pyruvate kinase isozymes, *Biochemistry 28*, 8756−8764.
10. Ibsen, K. H., and Trippet, P. (1974) Effects of amino acids on the kinetic properties of three noninterconvertible rat pyruvate kinases, *Arch. Biochem. Biophys 163*, 570−580.
11. Tsao, M. U. (1979) Kinetic properties of pyruvate kinase of rabbit brain, *Mol. Cell. Biochem. 24*, 75−81.

12. Reinhart, G. D. (1983) The determination of thermodynamic allosteric parameters of an enzyme undergoing steady-state turnover, *Arch. Bioch. Biophys. 224*, 389−401.

13. Johnson, J. L., and Reinhart, G. D. (1997) Failure of a two-state model to describe the influence of phosphor(enol)pyruvate on phosphofructokinase from *Escherichia coli*, *Biochemistry 36*, 12814−12822.

14. Wooll, J. O., Friesen, R. H., White, M. A., Watowich, S. J., Fox, R. O., Lee, J. C., and Czerwinski, E. W. (2001) Structural and functional linkages between subunit interfaces in mammalian pyruvate kinase, *J. Mol. Biol. 312*, 525−40.

15. Vagin, A., and Teplyakov, A. (1997) MOLREP: an automated program for molecular replacement, *J. Appl. Crystallogr. 30*, 1022−1025.

16. Collaborative Computational Project, Number 4 (1994) The CCP4 suite: programs for protein crystallography, *Acta Crystallogr. D. Biol. Crystallogr. 50*, 760−763.

17. Murshudov, G. N., Vagin, A. A., and Dodson, E. J. (1997) Refinement of macromolecular structures by the maximum-likelihood method, *Acta Crystallogr. D. Biol. Crystallogr. 53*, 240−55.

18. Emsley, P., and Cowtan, K. (2004) Coot: model-building tools for molecular graphics, *Acta Crystallogr. D. Biol. Crystallogr. 60*, 2126−32.

19. Winn, M. D., Isupov, M. N., and Murshudov, G. N. (2001) Use of TLS parameters to model anisotropic displacements in macromolecular refinement, *Acta Crystallogr. D. Biol. Crystallogr. 57*, 122−33.

20. Brunger, A. T. (1992) Free *R* value: a novel statistical quantity for assessing the accuracy of crystal structures, *Nature 355*, 472−475.

21. Laskowski, R. A., Macarthur, M. W., Moss, D. S., and Thornton, J. M. (1993) Procheck − a program to check the stereochemical quality of protein structures, *J. Appl. Crystallogr. 26*, 283−291.

22. Hilser, V. J., Dowdy, D., Oas, T. G., and Freire, E. (1998) The structural distribution of cooperative interactions in proteins: Analysis of the native state ensemble. *Proc. Natl. Acad. Sci. U.S.A. 95*, 9903−9908.

23. Mattevi, A., Valentini, G., Rizzi, M., Speranza, M. L., Bolognesi, M., and Coda, A. (1995) Crystal structure of *Escherichia coli* pyruvate kinase type I: molecular basis of the allosteric transition. *Structure 3*, 729−741.

24. Larsen, T. M., Benning, M. M., Rayment, I., and Reed, G. H. (1998) Structure of the bis(Mg2+)-ATP-oxalate complex of the rabbit muscle pyruvate kinase at 2.1 Å resolution: ATP binding over a barrel, *Biochemistry 37*, 6247−55.

25. Larsen, T. M., Benning, M. M., Wesenberg, G. E., Rayment, I., and Reed, G. H. (1997) Ligand-Induced domain movement in pyruvate kinase: structure of the enzyme from rabbit muscle with Mg2+, K+, and L-phospholactate at 2.7 Å resolution, *Arch. Biochem. Biophys. 345*, 199−206.

26. Walker, D., Chia, W. N., and Muirhead H. (1992) Key residues in the allosteric transition of *Bacillus* stearothermophilus pyruvate kinase identified by site-directed mutagenesis, *J. Mol. Biol. 228*, 265−276.

27. Fenton, A. W., Paricharttanakul, N. M., and Reinhart, G. D. (2003) Identification of substrate contact residues important for the allosteric regulation of phosphofructokinase from *Eschericia coli*, *Biochemistry 42*, 6453−6459.